ELSEVIER

Journal of Power Sources 57 (1995) 105–109

JOURNAL OF POWER SOURCES

Response of a solid oxide fuel cell to load change

Elmar Achenbach

Institute of Energy Process Engineering (IEV), Research Centre Jülich (KFA), 52425 Jülich, Germany

Received 23 June 1995; revised August 29, 1995

Abstract

The transient behaviour of a solid oxide fuel cell (SOFC) caused by load changes is investigated. For this purpose a step function of the current density is set to the fuel cell and the response of the cell voltage is calculated by applying a special SOFC simulation code. The relaxation time is strongly related to the transient temperature distribution of the solid cell structure. Therefore, it is in the order of some minutes depending on the design parameters and the operating conditions. As a remarkable result the cell voltage undershoots beyond the new steady-state value from where the relaxation process starts. This effect is discussed and explained. The transient process is generalized by introducing two dimensionless groups, the modified Fourier number, *Fo*, and the source term number, *So*. In terms of these characteristic numbers a simple relationship is derived to determine the relaxation time of arbitrary cell designs under arbitrary operating conditions.

Keywords: Solid oxide fuel cell; Simulation; Transient behaviour; Load change

1. Introduction

Load change is a frequently occurring transient process during solid oxide fuel cell (SOFC) plant operation. The control system has to react on such event. Therefore, knowledge about the response time of the stack is required.

A simulation code as described in Refs. [1,2] was applied to calculate the transient behaviour of the SOFC stack. It predicts the operating conditions for various design parameters in a spatial and temporal resolution.

The time-dependent change of the cell voltage caused by a jump function set to the current density is used as a criterion for the determination of the relaxation time, Δt. It is defined as the period necessary to recover 90% of the dynamic voltage drop resulting from the difference $U(t\rightarrow\infty) - U(t=+0)$.

For this study numerous transient computations have been performed. In order to cover a broad range of future applications the design and operating parameters have been varied widely. In particular, the dimension of the bipolar plate, the channel height and the properties of the solid material were changed by one order of magnitude. Furthermore, various assumptions for the fuel utilization, the stoichiometry factor and the current density have been applied. Finally, calculations without and with internal reforming have been conducted. In the latter case the fuel was a 30% pre-reformed gas resulting from a $H_2O/CH_4 = 2.5$ mixture at CO shift-equilibrium. The corresponding gas composition is:

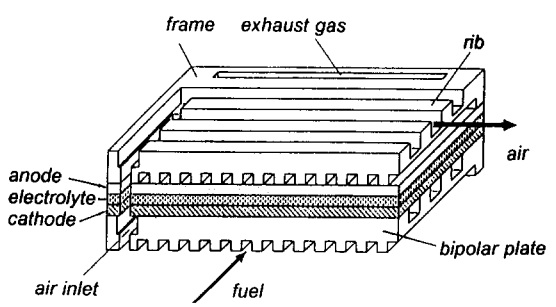

Fig. 1. Sketch of the planar solid oxide fuel cell.

$CH_4 = 17.10\%$, $H_2 = 26.26\%$, $CO = 2.94\%$, $CO_2 = 4.36\%$, $H_2O = 49.34\%$.

The only parameters to be unchanged are the active electrochemical area of 100 mm × 100 mm, the number of channels, $i_c = 20$, and the rib width $b_r = 2$ mm. In Fig. 1 a sketch of the cell design is depicted.

The computation of transient processes is CPU-time consuming, and not all design engineers have an appropriate code available. Therefore, an attempt was made to facilitate the prediction of the relaxation time by developing a simple algorithm. This is the subject of the second part of this contribution.

2. Computational results

In order to emphasize transient effects higher steps of the current density are applied in this study than usually will

SSDI 0378-7753(95)02263-4

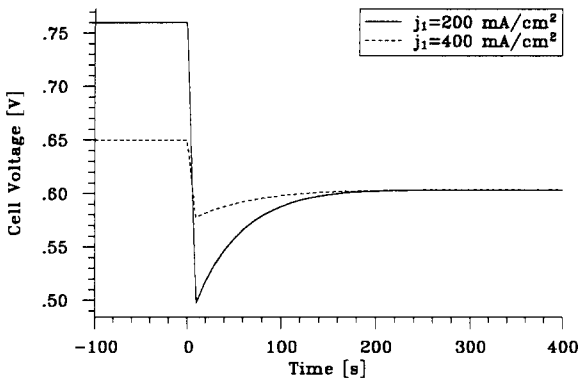

Fig. 2. Transient cell voltage during load change from j_1 to $j_2 = 500$ mA/cm^2; ceramic bipolar plate.

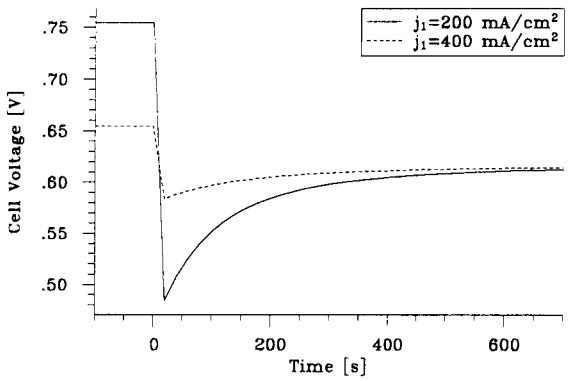

Fig. 3. Transient cell voltage during load change from j_1 to $j_2 = 500$ mA/cm^2; metallic bipolar plate.

occur during normal fuel cell operation. For this reason the cell must be supplied in advance with that amount of fuel which is required to achieve the new high performance at a given fuel utilization. Those calculations simulating a decreasing current-density step start with a given high utilization and reach a lower value for the new steady state.

Figs. 2 and 3 show the evolution of the cell voltage as a function of time for cells with ceramic or metallic bipolar plates, respectively. The configuration of both designs is identical. For $t < 0$ the cell voltage corresponds to the initial current density, j_1. The asymptotic value for $t \rightarrow \infty$ is the new steady-state cell voltage for the current density j_2. The intermediate period is characterized by an undershooting of the cell voltage, below the new steady-state value. The amount of the voltage drop correlates with the magnitude of the current-density step. The relaxation time, however, is independent of it.

The reason that the voltage indicates the undershoot effect is, that immediately after the jump ($t = +0$), the cell temperature is still low and related to the initial current density. The higher amount of waste heat produced at $j_2 = 500$ mA/cm^2 causes the cell temperature to increase which results in an increase in the cell voltage due to the decreasing internal cell resistance.

Figs. 2 and 3 demonstrate that the relaxation time depends on the design parameters of the cell, such as the solid material properties: the thermal conductivity, λ_s, the heat capacity, c_{ps}, and the density, ρ_s. Further parameters are the mass and the configuration of the solid structure and the waste heat produced. The ceramic cell, for instance, ($\lambda_s = 2$ W/(m K), $c_{ps} = 400$ J/(kg K), $\rho_s = 6600$ kg/m^3) needs about 120 s, the metallic ($\lambda_s = 27$, $c_{ps} = 500$, $\rho_s = 7800$) around 300 s to compensate for 90% of the dynamic voltage drop.

Fig. 4 demonstrates that the temporal variation of the cell voltage is closely related to the solid material temperature. The figure exhibits the maximum and minimum transient temperatures of the ceramic cell. The temperatures increase after the current-density jump and approach the value relevant for $j_2 = 500$ mA/cm^2. The response time of T_{max} nearly correlates with that of the cell voltage while the response time of T_{min} is about 2.5 times greater. The reason for this is associated with the counter-acting effects either of the endothermic steam reforming reaction or the exothermic electrochemical process as discussed below.

Fig. 5 shows the transient cell voltage as it may occur during operation of a large-scale power plant. A jump of the current density by 10%, from 270 to 300 mA/cm^2 is assumed. Now the waste heat production is lower as compared to preceding cases at 500 mA/cm^2. This results in a larger response time of $\Delta t = 220$ s. The undershooting voltage drop is only 6 mV.

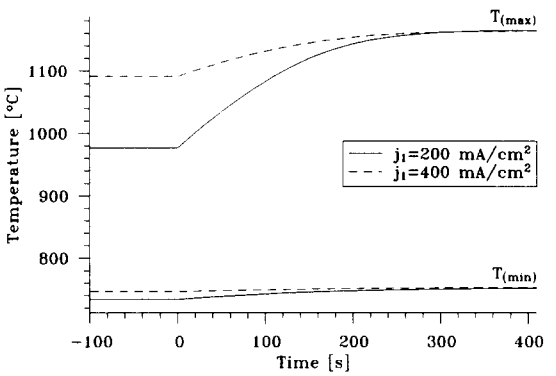

Fig. 4. Transient minimum and maximum solid temperature during load change from j_1 to $j_2 = 500$ mA/cm^2; ceramic bipolar plate.

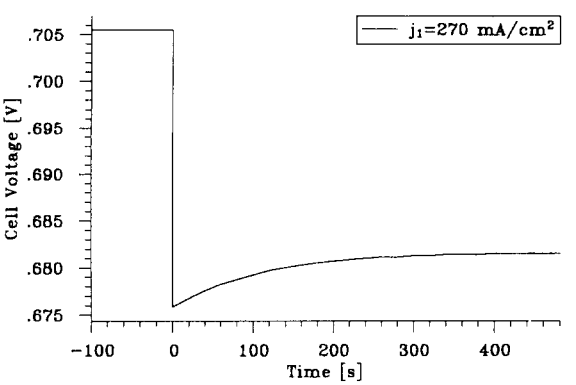

Fig. 5. Transient cell voltage during load change from $j_1 = 270$ to $j_2 = 300$ mA/cm^2. Ceramic bipolar plate.

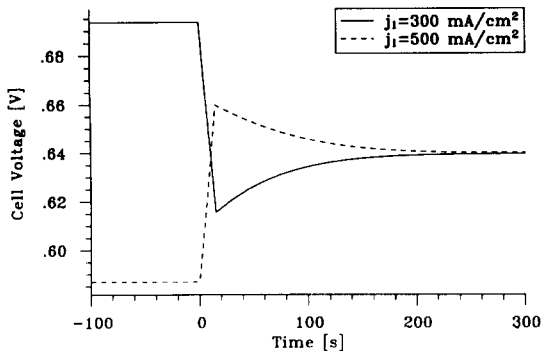

Fig. 6. Transient cell voltage during load change from $j_1 = 300$ or $j_1 = 500$ to $j_2 = 400$ mA/cm^2.

Finally Fig. 6 exhibits the transient cell voltage for the situation where the step of the current density is $+\Delta j$ and $-\Delta j$, respectively. Once the current density is set from $j_1 = 300$ mA/cm^2, once from $j_1 = 500$ mA/cm^2 to the new steady-state value of $j_2 = 400$ mA/cm^2. Though the curves are not symmetric with respect to the horizontal line through the new steady-state voltage value, the response times are the same.

3. Evaluation of the computational results

In order to adjust the determination of the relaxation time to the design engineer's requirements an attempt was made to facilitate the prediction procedure by introducing a simple algorithm. For this purpose the governing parameters must be identified.

Since all chemical, fluid dynamic and mass-transfer processes are fast compared with the dissipation of heat in the stack, the dynamic term must only be considered in the energy balance of the solid structure. This means that a quasi steady-state solution of the problem is achieved at each time step except for the temperature of the solid phase.

Eq. (1) represents the energy balance of the solid:

$$(\rho c_p)_s \frac{\partial T_s}{\partial t} = \lambda_{eff,x} \frac{\partial^2 T_s}{\partial x^2} + \lambda_{eff,y} \frac{\partial^2 T_s}{\partial y^2} + \lambda_{eff,z} \frac{\partial^2 T_s}{\partial z^2} + \Phi \quad (1)$$

where T_s is the local solid temperature. The thermal conductivities, λ_{eff}, of the quasi-homogeneous stack structure are effective quantities which must separately be determined for each of the spatial coordinates according to Ref. [1]. Since the effective thermal conductivity includes the contributions of heat conduction through the solid and gaseous phase and of radiation it is a non-isotropic and strongly temperature-dependent property.

The sum of the heat rates produced or consumed in the chemical and electrochemical processes and those transferred from the fuel and the air to the walls occur as the source term, Φ.

Eq. (1) can be written dimensionless by introducing the following quantities:

$$\Theta = \frac{T - T_E}{T_O - T_E}; \quad \tau = \frac{t}{\Delta t}; \quad \xi = \frac{x}{h_{eff}};$$

$$\eta = \frac{y}{h_{eff}}; \quad \zeta = \frac{z}{h_{eff}} \quad (2)$$

where $\Delta T = T_O - T_E$ is the difference of the outlet and entrance temperatures of the cooling air stream. The quantity Δt means a characteristic time interval which is in the present case the relaxation time. As a characteristic length scale the effective thickness of the solid structure, h_{eff}, occurs, defined in Eqs. (3) and (4):

$$h_{eff} = (1 - \epsilon)(d_{PEN} + d_b + h_a + h_f) \quad (3)$$

$$\epsilon = 1 - \frac{d_{PEN}(\rho c_p)_{PEN} + (\rho c_p)_b \left[d_b + \frac{b_r}{b_r + b_c} (h_a + h_f) \right]}{(\rho c_p)_{PEN} d_{PEN} + (\rho c_p)_b (d_b + h_a + h_f)} \quad (4)$$

The explanation of the symbols can be read from Fig. 7.

The total specific waste heat, P_w, to be removed from the cell can be expressed by the electric specific output P_c of the cell and the efficiency η_c:

$$P_w = P_c(1 - \eta_c)/\eta_c = Uj(1 - \eta_c)/\eta_c \quad (5)$$

Eq. (1) yields together with Eqs. (2) and (5) the dimensionless form of the energy balance of the solid:

$$\frac{\partial \Theta}{\partial \tau} = \frac{\lambda_s \Delta t}{(\rho c_p)_s h_{eff}^2} \left(\frac{\lambda_{eff,x}}{\lambda_s} \frac{\partial^2 \Theta}{\partial \xi^2} + \ldots \frac{1 - \eta_c}{\eta_c} \frac{Uj}{\lambda_s \Delta T / h_{eff}} \right) \quad (6)$$

The solution of Eq. (6) depends on two dimensionless groups. The first is the Fourier number, Fo, formed with the effective height, h_{eff}, of the cell structure.

$$Fo = \lambda_s \Delta t / [(\rho c_p)_s h_{eff}^2] \quad (7)$$

The second group derives from the source term and is called, therefore, the source term number, So:

$$So = Uj(1 - \eta_c)/(\eta_c \lambda_s \Delta T / h_{eff}) \quad (8)$$

Its physical meaning is the ratio of two heat fluxes, i.e. the waste heat flux compared with a heat flux resulting from heat

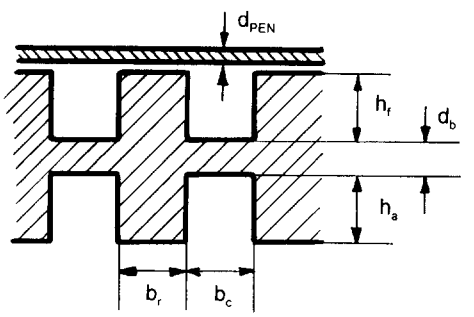

Fig. 7. Sketch of the SOFC solid structure.

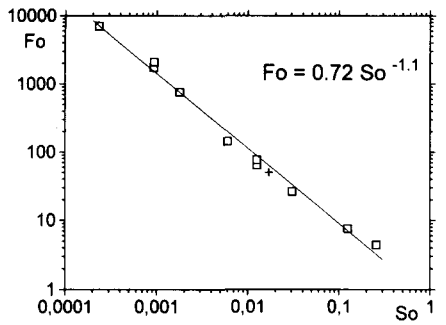

Fig. 8. Fourier number, *Fo*, vs. source term number, *So*. Computational result and approximation algorithm: (+) start-up procedure.

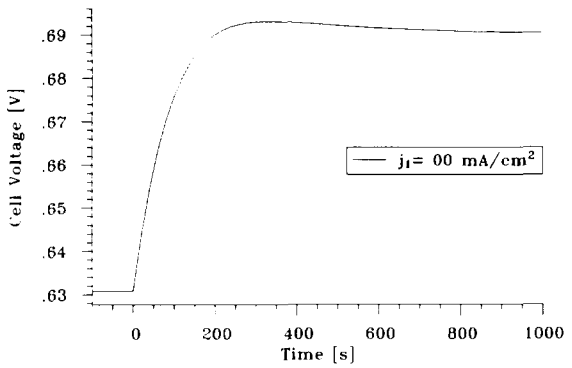

Fig. 9. Transient cell voltage during start-up procedure of a ceramic cell. Current density step from $j_1 = 0$ to $j_2 = 300$ mA/cm^2.

conduction through a plate when h_{cff}, is its thickness, λ_s its thermal conductivity and ΔT the temperature difference.

As mentioned above numerous calculations of load change processes have been performed to reveal the relationship between *Fo* and *So*. For this purpose the relevant parameters such as $(\rho c_p)_s$, λ_s, h_{cff}, ΔT and *Uj* have been varied within one order of magnitude to cover a wide range of applications. The result is shown in Fig. 8. The data can be approximated by a simple equation:

$$Fo = 0.72 So^{-1.1} \tag{9}$$

Since the *So* number, Eq. (8), only contains known design data, the *Fo* number can be determined from Eq. (9) and hence the relaxation time, Δt.

The start-up procedure of a stack appears as a special case of the load change. Here, the current density starts from $j_1 = 0$ and is instantaneously set to an amount of j_2 which is chosen in the present example to be $j_2 = 300$ mA/cm^2, for instance. Fig. 9 shows the temporal development of the cell voltage for a ceramic cell heated up to a temperature of 900 °C before the current density j_2 is demanded. Within about 200 s the cell voltage reaches the maximum followed by a minor gradual decrease until the final steady state is established after about 900 s. 90% of the voltage difference is recovered after a time interval of $\Delta t = 150$ s which is the relaxation time in the present definition. This result expressed in terms of *Fo* and *So* numbers is indicated in Fig. 8 by the cross symbol.

The development of the whole temperature field during the start-up procedure is given in Fig. 10. The particular pictures for the period up to 160 s indicate a continuous change of the isotherm pattern. For an elapsed time greater than 160 s the change is no longer essential and a uniform temperature across the cell is nearly established. Only the maximum and particularly the minimum are observed to be more pronounced (see also Fig. 11) at longer relaxation times. Due to the effect of the slowly relaxing temperature minimum the average temperature decreases slightly resulting in a minor diminution of the cell voltage.

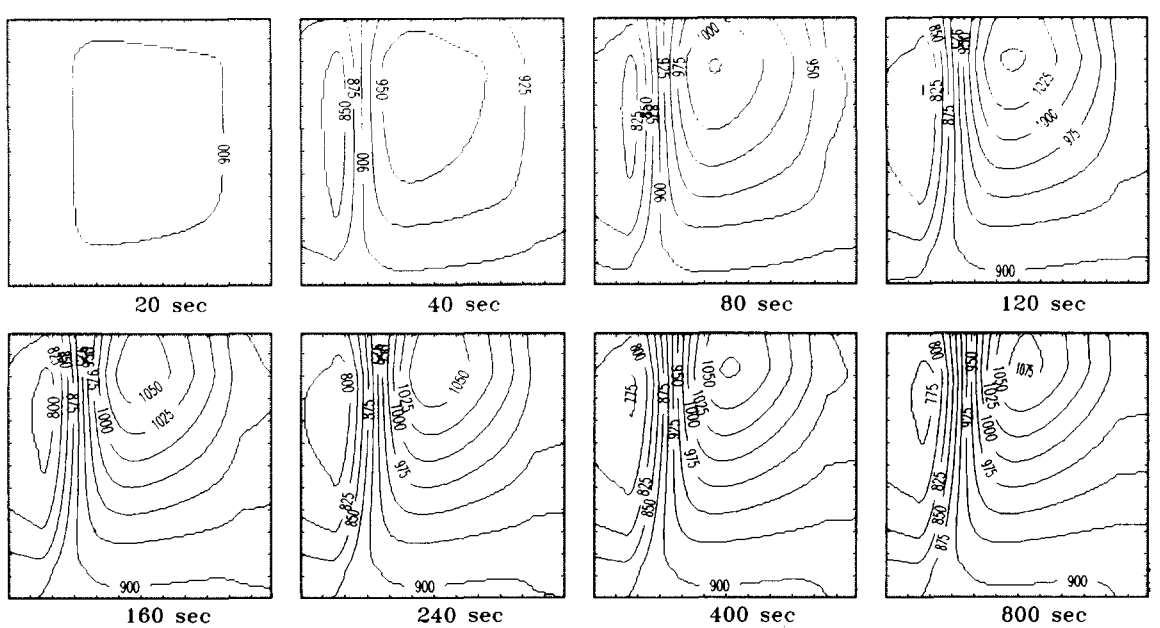

Fig. 10. Transient temperature field during start-up procedure of a ceramic cell. Current density step from $j_1 = 0$ to $j_2 = 300$ mA/cm^2. Fuel from left, air from below.

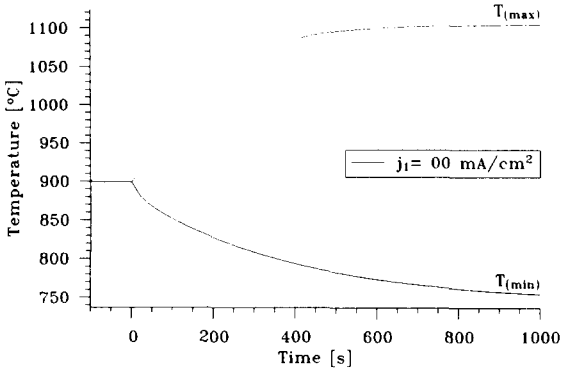

Fig. 11. Transient minimum and maximum solid temperature during start-up procedure of a ceramic cell. Current density step from $j_1 = 0$ to $j_2 = 300$ mA/cm^2.

4. Conclusions

The transient behaviour of a solid oxide fuel cell during load change is treated theoretically. The relaxation time is calculated for the situation where an immediate step function is set to the current density. The response of the cell to the increase in performance is discussed with a view to the temporal development of the cell voltage. The computational data show that an undershoot of the cell voltage occurs followed by a relaxation process. Some minutes are necessary to establish new steady-state conditions. This relaxation process is closely related to the transient temperature distribution of the solid cell structure, since the internal cell resistances are strongly temperature dependent. Thus, the relaxation time depends on the thermal properties, size and configuration of the cell, and on the operating conditions.

An attempt is made to facilitate the prediction of the relaxation time by introducing two characteristic numbers. These are the modified Fourier number, *Fo*, and the source term number, *So*. In terms of these dimensional groups the following simple relationship is proposed to solve this problem.

$$Fo = 0.72 So^{-1.1}$$

The start-up procedure is recognized to be a special case of the load change process.

5. List of symbols

b	width (m)
c_p	heat capacity (kJ/(kg K))
d	thickness (m)
Fo	Fourier number, Eq. (7)
h	height (m)
j	current density (A/m^2; mA/cm^2)
P_e	specific electric power (W/m^2)
P_w	specific waste heat flux (W/m^2)
So	source term number, Eq. (8)
t	time(s)
T	temperature (K)
U	cell voltage (V)
x, y, z	coordinate (m)

Greek symbols

ϵ	porosity
Θ	dimensionless temperature
ζ, η, ξ	dimensionless coordinates
η_e	electric efficiency related to upper heating value and fuel converted
λ	thermal conductivity (W/(m K))
Φ	source term (W/m^3)
ρ	density (kg/m^3)
τ	dimensionless time

Subscripts

b	bipolar plate
c	gas channel
eff	effective
E	entrance
O	outlet
PEN	PEN structure (anode, electrolyte, cathode)
s	solid structure

References

[1] Ch. Rechenauer and E. Achenbach, Dreidimensionale mathematische Modellierung des stationären und instationären Verhaltens oxidkeramischer Hochtemperatur-Brennstoffzellen, *Jül.-Rep. 2752*, Apr. 1993.

[2] E. Achenbach, *J. Power Sources, 49* (1994) 333–348.